

Corrosion of Carbon Steel in Presence of Hydrocarbon

L. D. López León^{1,2}, M. A. Veloz Rodríguez^{1*}, V. E. Reyes Cruz¹, F. Almeraya Calderón²,
S. A. Pérez García²

¹ Universidad Autónoma del Estado de Hidalgo, Carr. Pachuca Tulancingo Km 4.5, Col Carboneras,
Mineral de la Reforma, Hgo. México C.P. 42184

² Centro de Investigación en Materiales Avanzados, Miguel de Cervantes 120, Complejo Industrial
Chihuahua, Chihuahua, Chih. Mexico C.P. 31109

*E-mail: mveloz@uaeh.edu.mx

Received: 29 April 2011 / Accepted: 5 July 2011 / Published: 1 August 2011

In this work the study of the behaviour AISI 1018 in a buffered solution like NACETM177 with and without hydrocarbon. Polarisation curves indicated slopes changing with the hydrocarbon presence enhancing the reduction reaction and inhibiting oxidation. EIS technique shows high activity of steel in the solution at low frequencies, establishing that interaction of the ions in solution with the metal is enhanced by hydrocarbon, where the adsorption processes are governing the corrosion mechanism. The adsorption of corrosive agents prevents the formation and growth of a passive layer, even in the presence of hydrocarbon and the corrosion rate is high.

Keywords: Carbon steel, acetic acid, chloride, polarisation curves, electrochemical impedance spectroscopy, Adsorptive processes

1. INTRODUCTION

A common method used for evaluation of metallic materials subject to stress and / or blistering in the oil industry is the NACE TM 0177 [1]. This method uses a highly corrosive environment in contact with the materials to be evaluated. The high aggressiveness of the media is adequate for reliable results in a short time. Also, it has a high hydrogen concentration and low pH, which is commonly found in primary distillation of refinery plants. On the other hand, organic acids and chlorides cause corrosion resulting in a more complex phenomenon.

Previously, it has been reported [2] the corrosion mechanism in a system with AISI 1018 carbon steel in a buffered solution like NACE TM 0177, establishing that the interaction of acetic acid, acetate and chlorides with the metal (where the adsorption processes are governing the corrosion mechanism), could be modified by the presence of other faces such as hydrocarbon as occurs in the

petroleum industry. So, in order to find the effect of immiscible mixtures on the corrosion of the carbon steel, in this work is studied its behaviour in a solution like NACE TM 0177 in absence and in presence of hydrocarbon (kerosene).

2. EXPERIMENTAL

A typical three-electrode cell setup was used in electrochemical techniques with a Hg/HgCl(s)/KCl(sat) electrode as reference and a graphite bar as counter electrode. As working electrodes discs of low carbon steel AISI 1018 (C 0.15/0.20%; Mn 0.60/0.90%; Si 0.15/0.30%; P max. 0.04%; S max. 0.05%) were used and coupled to a Teflon support. Prior to each experiment, electrode surface was abraded with 280 SiC emery paper.

The corrosive environment equivalent to the method used in NACE TM 0177 [1], has the following composition: 0.04M CH₃COOH / NaCOOCH₃, pH = 3.5, 30172 ppm Cl⁻ as NaCl (0.52 M Cl⁻) in the absence and presence of kerosene (20%_{v/v}). The solution was prepared with deionized water, deaerated with high purity nitrogen for 30 min. The following reagents were used (A. R. grade): 99% purity NaCl Baker; 100% purity CH₃COOH glacial Merck, 99% purity CH₃COONa*3H₂O Baker and kerosene (hydrocarbon) from Baker. Buffered solution is used to avoid, as much as possible, the change in pH and the consequent change of experimental conditions.

All experiments were performed at 25°C and after 10 minutes of immersion of the working steel electrode, to allow the corrosion potential stabilization. The potentiodynamic polarisation curves were registered at scan rate of 0.1mV/s in a potential range between ± 300 mV (vs. o.c.p.) and each curve was obtained from a freshly polished steel surface.

The electrochemical impedance spectroscopy (EIS) measurements were carried out with an amplitude of 10 mV (vs. o.c.p.) and in the frequency range of 10 mHz to 10 kHz. A Frequency Response Analyser (FRA), coupled to a Potentiostat-Galvanostat Autolab Mod PGSTAT30 and managed through the software of the same company.

It is important to stress that all electrochemical experiments were carried out under hydrodynamic conditions, using a mechanic stirrer at 2000 rpm in order to achieve a homogeneous emulsion when kerosene was introduced in the model solution.

3. RESULTS

3.1. Polarisation curves

The figure 1 shows the Potentiodynamic polarisation curves of AISI 1018 carbon steel in the acetic model solution (curve i) and in the emulsion of kerosene (curve ii). It can be seen that the presence of kerosene (curve ii) increases the cathodic reaction rate (associated with hydrogen evolution), but diminishes the anodic one, it means the steel active dissolution.

In the analysis of polarisation curves, the system in the presence of hydrocarbon shows a greater R_p value than the system free of hydrocarbon. This value indicates an effect of inhibition by either the presence of non-conductive compounds or the increase in competition with the adsorption of corrosive agents.

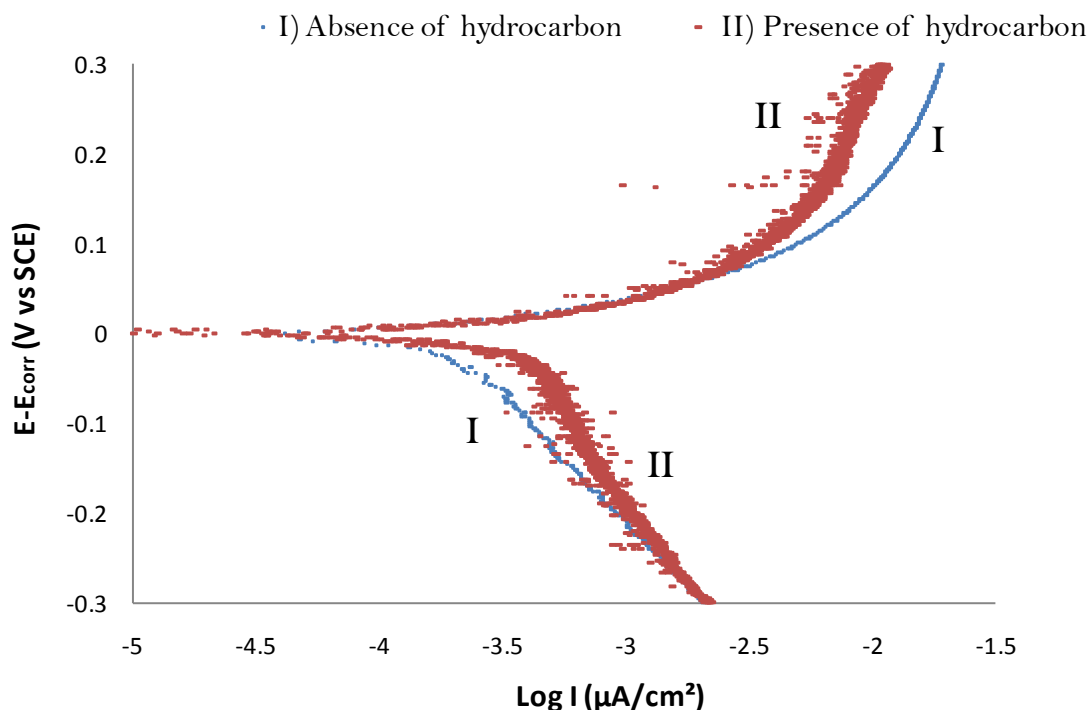


Figure 1. Potentiodynamic polarisation curves obtained with a scan rate of 0.1 mV/s, on AISI 1018 carbon steel in a buffered solution of Ac/Ac^- pH 3.5, 30,172 ppm Cl^- in I) presence and II) absence of hydrocarbon.

The specific adsorption of acetate ions and Cl^- in the corrosive environment [3] appears to be modified by the hydrocarbon, favouring its arrival to the metal surface which is shown in the increase of the cathodic current. However, there are also diffusive processes that become more important with the presence of hydrocarbon, which is manifested in a larger increase in the cathodic slope.

This fact suggests that the presence of hydrocarbon modifies the diffusive processes, since the cathodic slope values increase rapidly from potential values near the corrosion potential showing non-Tafel behaviour. That was the reason to calculate slopes in the potential range of $E_{\text{corr}} \pm 60$ mV and R_p in the range of $E_{\text{corr}} \pm 15$ mV. The characteristic parameters of polarisation curves are present in Table 1. It shows that the anodic reaction was not modified with the presence of kerosene since the anodic slope values are very similar between them, but the cathodic one change with kerosene being more active and it is evident with the corrosion current values found. Table 2 presents corrosion current values obtained for the different systems reported in the literature and the system under study (acetic acid, NaCl and hydrocarbon).

Table 1. Corrosion parameters obtained for the different systems

	E_{corr}	$R_p (\pm 15\text{mv})$	ba	bc
Acetic acid, NaCl	-0.59 V	77.48 Ω/cm^2	0.035 V/dec	-0.092 V/dec
Acetic acid, NaCl and Hydrocarbon	-0.59 V	56.32 Ω/cm^2	0.033 V/dec	-0.044 V/dec

The analysis of the I_{corr} reveals that the presence of H_2S or hydrocarbon (kerosene) significantly increases the steel corrosion current density in acetic acid which contains chloride (NaCl) and thus, the steel corrosion rate is higher in three orders, compared to that in acetic acid (Table 2). Comparing with the system with acetic acid, NaCl and H_2S , the current density is lower but not significantly because of their similar order of magnitude. This is important due to the fact that presence of hydrocarbon favours the specific adsorption of acetate and Cl^- ions to the metal surface.

Table 2. Corrosion parameters obtained for the different systems

Solution	$I_{\text{corr}} (\text{A}/\text{cm}^2)$
Acetic acid [2]	1.62×10^{-07}
Acetic acid, NaCl *	8.0×10^{-05}
Acetic acid, NaCl and H_2S [2]	7.54×10^{-04}
Acetic acid, NaCl and Hydrocarbon *	1.07×10^{-04}

* This work.

3.2. Electrochemical Impedance Spectroscopy

Electrochemical impedance spectroscopy was carried out in order to establish the number of stages involved in both, the anodic and cathodic processes. This technique was used to obtain the electrochemical characteristics of the corrosion mechanism and to separate the contributions of different phenomena, which interfere and control the carbon steel corrosion process.

The results showed that steel surface is active (figure 2), since the values of real and imaginary impedances are lower compared to the work previously reported [2].

The registered impedance spectra (Fig.2) shows that the corrosion steel is controlled by charge transfer mechanism in the studied model solution, however in the presence of kerosene the EIS reveals negative inductive loop at lower frequencies than 1Hz. This fact could be attributed to adsorption of some species [3] part of the solution or corrosion products formed on the steel surface. Besides, the semicircle shows increased value of impedance with kerosene and lower polarisation resistance. These data correlate well with the reported polarisation curves (Fig.1), indicating a higher steel corrosion current (Table 1 and Table 2) in the system due to the presence of kerosene.

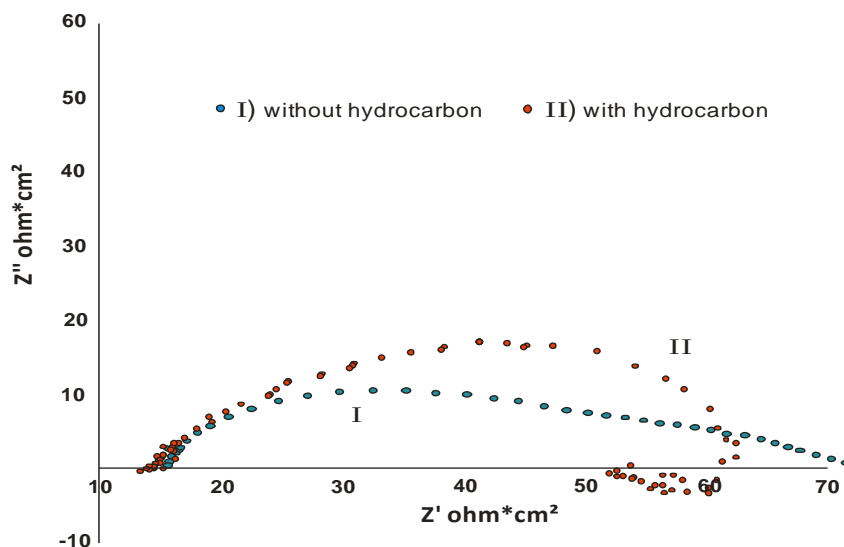


Figure 2. Typical Nyquist diagrams obtained for the system I) without and II) with hydrocarbon on carbon steel in a buffered solution of Ac/Ac⁻ pH 3.5, 30,172 ppm Cl⁻, at frequency range of 10 mHz to 10 KHz.

3.2.1. Electrochemical impedance with imposed potential

Figure 3 and Figure 4 present the Nyquist diagrams of low carbon steel AISI 1018 registered in the model acetic solution, in the presence of kerosene (hydrocarbon), through the imposition of different values of anodic (Fig.3) and cathodic polarisation (Fig.4), from 10 to 50 mV vs. the open circuit potential.

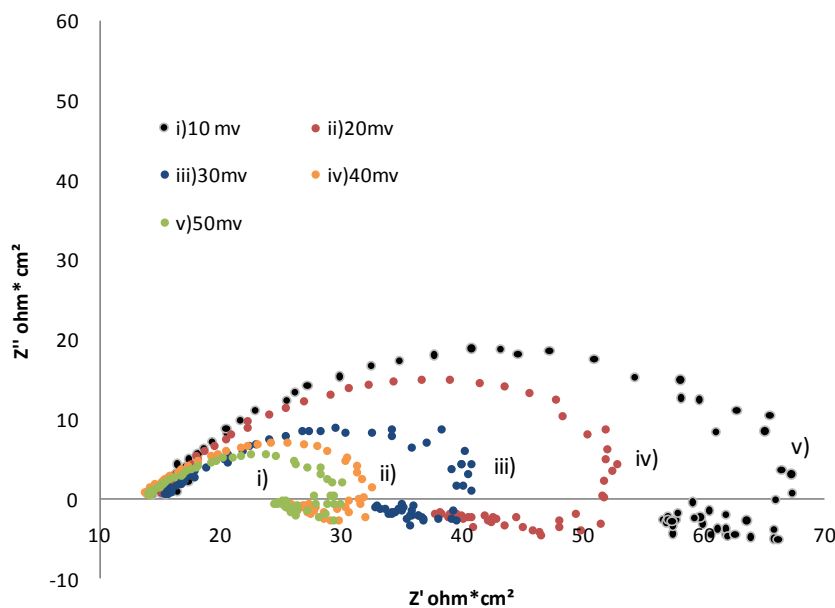


Figure 3. Typical Nyquist diagrams obtained for the carbon steel in a buffered solution of Ac/Ac⁻ pH 3.5, 30,172 ppm Cl⁻, varying the imposed potential i) E_{corr} + 10mV, ii) E_{corr} + 20mV, iii) E_{corr} + 30mV, iv) E_{corr} + 40mV and v) E_{corr} + 50mV in a frequency range of 10 mHz - 10 kHz.

It can be seen that the different values of imposed polarisation cause an immediate change in the shape of the impedance spectra and its characteristic parameters. However, the effect of anodic and cathodic polarisation on the EIS curves is different.

For example, the increment of the applied anodic polarisation (Fig.4) diminishes abruptly the polarisation resistance (real impedance) and imaginary one (reactance) values, with the tendency to form more clearly an inductive loop in the E at low frequencies in the EIS spectra.

Nevertheless, the increment of the applied cathodic polarisation (Fig.5) affects showing higher resistance polarisation and reactance values, forming clear inductive loop at higher frequencies and at the highest cathodic polarisation of 50 mV. The inductive loop could be attributed to adsorbed species present in the solution with kerosene or as a part of the steel corrosion products. The different frequencies, lower and higher respectively for the anodic (Fig.4) and cathodic (Fig.5) loops, may indicate a competition in the adsorption of species, or the fact that the inductive effect is becoming less important. These effects could be associated also with diffusive processes in the agitated kerosene – model solution (emulsion) as high speed results in a stable layer near to the electrode surface. The registered Nyquist diagrams also confirmed the effects discussed above.

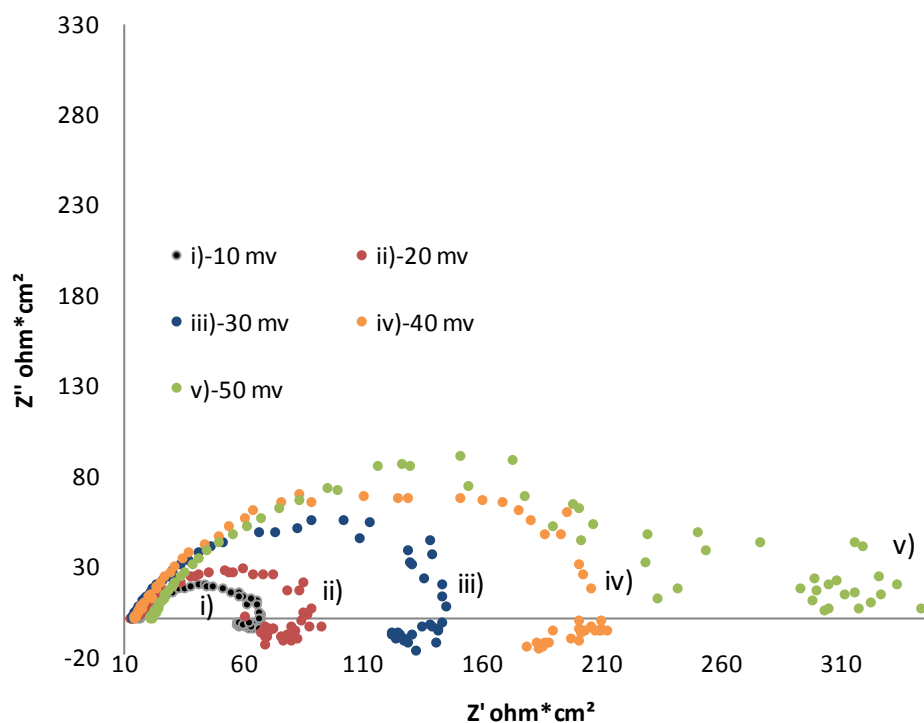


Figure 4. Typical Nyquist diagrams obtained for the carbon steel in a buffered solution of Ac/Ac^- pH 3.5, 30,172 ppm Cl^- , varying the imposed potential i) $E_{\text{corr}} - 10\text{mV}$, ii) $E_{\text{corr}} - 20\text{mV}$, iii) $E_{\text{corr}} - 30\text{mV}$, iv) $E_{\text{corr}} - 40\text{mV}$ and v) $E_{\text{corr}} - 50\text{mV}$ in a frequency range of 10 mHz - 10 kHz.

The Nyquist diagrams obtained by imposing anodic over potentials have similar behaviour at high frequencies (10 kHz to 100 Hz). As the imposed potential increases only a decrease in magnitudes of the total impedances is observed, indicating a decrease in polarisation resistance.

Nyquist diagrams obtained (Figure 3) exhibit an inductive loop at low frequencies, indicating the adsorption and desorption of species at the electrode surface. Kedam and colleagues [3] have found this type of inductive loops in the anodic dissolution of iron in acidic environment, attributing it mainly to the number of adsorbed species and the relaxation process where the potential is imposed. Moreover, the negative over potential (Figure 4) in the Nyquist diagram showed a change in the shape of the inductive loop, increasing the total impedance and showing a similar behaviour at high frequencies.

The series of points at low frequencies differ from those seen at the anodic over potential, it may indicate a competition in the adsorption of species, or that an inductive effect is becoming less important. These points could be associated with diffusive processes (of H^+ , Cl^- or Ac^- , or all together) and the electrode which is in an agitated emulsion at high speeds resulting in a stable layer near to the electrode surface.

By increasing the potential difference, the values of the real and imaginary impedance increase, unlike to what was observed when faced with a more positive potential. This indicates that, the cathodic process generates products which slow down the charge transfer and that are associated to a competitive adsorption between Ac^- and Cl^- .

4. DISCUSSION OF EIS EXPERIMENTAL RESULTS

In order to perform a quantitative analysis of the impedance spectra, EIS diagrams obtained from both solutions were simulated with the equivalent circuit, shown in Figure 5. Some authors have used a circuit similar to discuss the influence of hydrogen sulphide on corrosion of iron [4,5] in acidic environment and hydrogen permeation of steel, studied by electrochemical techniques [6,7]. The reported results allowed them to consider not only the inductive part of the EIS spectra.

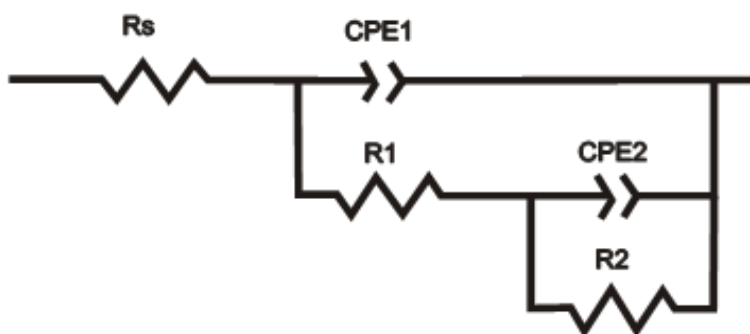


Figure 5. Equivalent circuit used to simulate impedance diagrams obtained for a carbon steel system SAE 1018 (rotation speed 2000 rpm) in a 0.04M HAc/Ac⁻ solution, pH = 3.5, 30,172 ppm Cl⁻ in the presence of hydrocarbon.

In our study the interpretation of some EIS parameters was performed by adjusting the spectra using the Zview2 program, and the physical interpretation proposed by other authors [4,6]. The circuit (Figure 5) allows identifying the solution resistance (R_s) and charge transfer resistance (R_1). The EIS

diagrams (Figs.3-4) showed that the steel double layer capacitance is affected by some imperfection on the electrode surface, which is simulated using a constant phase element (CPE1) [5,6]. The parameter n of the CPE2 is negative indicating the presence of adsorptive processes [4,7].

Table 2 shows the representative values for the resistances, obtained from the best fitting of the EIS experimental data, using the equivalent circuit (Fig.5): solution resistance (R_s), charge transfer (R_1) and adsorptive resistance (R_2), at all polarisation values, anodic and cathodic. The solution resistance (R_s) at the steel surface shows relatively similar values, influenced principally by the presence of kerosene near the electrode, as a part of the formed emulsion. When imposing more negative potential than E_{corr} , there is a tendency of R_1 and R_2 to increase as the imposed potential becomes more negative, whereas towards more positive potential than E_{corr} , R_1 and R_2 decrease. Thus, it could be proposed that the predominant phase in the corrosion process seems to be a stage associated with oxidation. Moreover, the positive overpotentials, show that R_1 and R_2 have a greater value than the corrosion potential, diminishing by increasing the potential difference $E_{corr} - E_{imp}$. Towards negative overpotentials the same behaviour is observed, suggesting that the imposed potential causes a diminution of the quantity of adsorbed species. Nevertheless, the analysis of constant phase elements associated to the resistances in R_1 and R_2 , CPE1-CPE2, arrangements is necessary.

Table 3. Resistances and constant phase elements for the data calculated through the best fit of experimental data to the equivalent circuit in Figure A.

E- E_{corr} (mV)	Resistances (Ω)			CPE1		CPE2	
	R_s	R_1	R_2	$Y_o \times 10^{-5}$ ($\Omega^{-1}s^n$)	n_1 (0 – 1)	Y_o ($\Omega^{-1}s^n$)	n_2 (0 – 1)
10	14.62	11.26	25.02	62	0.7634	0.1023	-0.4311
20	14.22	17.96	29.41	56	0.7733	0.0896	-0.4234
30	14.97	18.63	35.4	52	0.7784	0.0986	-0.6254
40	15.47	19.77	42.85	78	0.6878	0.1027	-0.5926
50	14.5	21.76	53.05	77	0.6400	0.1112	-0.4115
0	14.97	35.12	65.41	53	0.7285	0.0952	-0.5213
-50	14.61	51.43	83.01	71	0.6650	0.0838	-0.6070
-40	14.87	66.4	130.12	37	0.7943	0.0867	-0.5216
-30	14.07	78.1	150.23	33	0.7770	0.1333	-0.4122
-20	14.23	90.05	170.21	55	0.7301	0.0989	-0.4533
-10	15.01	105.1	185.86	42	0.7011	0.1163	-0.5231

Table (3) shows the values of the constant phase elements obtained for the best fitting of experimental data to the equivalent circuit in Figure 5. It is observed that the values of n_1 , for the CPE1 obtained at different potentials imposed are very similar (about 0.65-0.75) and can be attributed mainly to the roughness of the electrode surface. Values of Y_0 have high similarities indicating the modification of the steel - electrolytic environment interface. In the case of CPE2, it is important to

point out that all calculated n are similar in magnitude, validating the assumption that these elements are associated to the adsorption of species. The negative sign of these values is attributed to the CPE2 as an inductor and not as a capacitor, which is consistent with the physical interpretation given to adsorptive processes [8,9].

In studies of systems containing HAc/Ac^- [7,9,10] it has been proposed that the corrosion mechanism occurs through adsorption of HAc at the metal surface, but the values of the anodic slopes reported in this work are affected by the conductivity of the solution, the presence of other ions and in general by other experimental conditions. In this way, in literature [11,12] anodic Tafel slopes are 106 mV/decade and they attributed the difference in slopes based on other studies (29 mV/decade) [13, 14] to the treatment provided to the electrodes before performing the experiments, which would change the mechanism.

On the other part, the slopes of polarisation curves obtained through the whole anodic branch are similar to those obtained by Nord and Bech-Nielsen [10] where it is proposed that, given the initial presence of a layer of ferric ions at the metal surface and since the coordination number of these, the number of acetate ions adsorbed on a surface iron atom in its active state, should not be more than two, thus obtaining a slope of 90 mV/decade.

This agrees with the anodic slope values similar to those obtained by Nord and Bech-Nielsen, and with the anodic behaviour of the impedance diagrams, the difference is observed only in the adsorptive process.

Some authors agree that the output of a proton from the adsorbed acetic acid governs the rate of corrosion and, since the chloride adsorption on the metal surface is slower than that of acetate ions [15, 16, 17] is feasible to think that in anodic conditions, the mechanism is by adsorption of the latter.

The role of chlorides in the system can be through two mechanisms: the promotion of corrosion or inhibition [18, 19, 20], implying that the chloride in the solution has an important role in the dissolution process [21]. However, in the present work their effect is not appreciated on the corrosion mechanism, as it was stated in literature [2].

Hence, one can establish that the general mechanism of anodic process for the system under study is similar to that proposed by Nord and Bech-Nielsen [10], where metal dissolution occurs primarily by adsorption without charge transfer of ions Ac^- , which is further emphasized by the presence of hydrocarbon.

For the cathodic process, Singh and Gupta [8] found cathodic slopes of more than 300mV/decade (as in this work when all the cathodic values are considered), reporting that the behaviour of polarisation curves in a system HAc/Ac^- indicate that the cathodic reaction and its mechanism are the following:



Thus the overall mechanism involves the HAc diffusion through the film of hydrocarbon, the adsorption of HAc , acetate production and evolution of H_2 which is confirmed experimentally in the

curves of cathodic polarisation where slopes have high values and the impedance spectra show the predominance of both the adsorptive and diffusive process by showing a flattened shape [22, 23].

5. CONCLUSIONS

The analysis of the values of I_{corr} showed that the presence of hydrocarbon increases the current density and the corrosion rate, compared to the system with acetic acid and NaCl. The presence of hydrocarbon amends the specific adsorption of acetate and Cl^- ions, favouring their arrival to the metal surface. Using the electrochemical impedance spectroscopy (EIS) technique, in combination with the results of polarisation curves it was possible to propose a mechanism to represent the corrosion of carbon steel AISI 1018 in an environment of acetic acid, chlorides and kerosene. In the proposed mechanism, the adsorption of acetic acid remains decisive for the process. The chlorides appear to act only in secondary reactions or corrosion products. The interaction of acetic acid, acetate and chlorides with the metal is increased by the presence of hydrocarbon substantially modifying the corrosion rate of the system, where adsorption processes are ruling and leading to corrosion rates similar to the system in the presence of H_2S . The adsorption of corrosive agents prevents the formation and growth of a passive layer of corrosion products; thus, the obtained corrosion rates are higher.

ACKNOWLEDGMENTS

To PROMEP by the project UAEHGO-PTC-293 and CONACYT for Basic Science project 00023889, these provided financial resources to acquire the infrastructure used in this work. To Prfrs. Mark Jeannin and Lucien Veleva for their useful revisions to this work.

References

1. Method Standard NACE TM 0177 *Laboratory Testing of Metals for resistance to specific forms of environmental cracking in H₂S*, NACE, (1996).
2. M.A. Veloz, I. Gonzalez, *Electrochim. Acta*, 48 (2002) 135-144.
3. Kedam M., Mattos O. R., Takenouti H., *J. Electrochem. Soc.*, 128 (1981) 257.
4. H. Ma, X. Cheng, G. Li, S. Chen, Z. Quan, S. Zhao, L. Niu, *Corros. Sci.*, 42 (2000) 1669.
5. J.M. Bastidas, P. Pinilla, J.L. Polo, E. Cano, *Corrosion.*, 58 (2002) 922.
6. C. Azevedo, P. S. A. Bezerra, F. Esteves, C. J. B. M. Joia, O. R. Mattos, *Electrochim. Acta*, 44 (1999) 4431.
7. X. Y. Zhang, S.B. Lambert, R. Sutherby and A. Plumtree, *Corrosion*, 55 (1999) 297-305.
8. M. M. Singh, A. Gupta, *Corrosion*, 56 (2000) 371.
9. B.Y. Fang, A. Atrens, J.Q. Wang, E.H. Han, Z.Y. Zhu and W. Ke, *Journal of Materials Science.*, 38 (2003) 127-132.
10. H. Nord, G. Bech-Nielsen, *Electrochim. Acta*, 16 (1971) 849.
11. D. Wang, S. Li, M. Wang, H. Xiao, Z. Chen, *Corros. Sci.*, 41 (1999) 1911.
12. K. A. Christiansen, H. Hoeg, K. Michelsen, G. Bech-Nielsen, H. Nord, , *Acta Chem. Scand.*, 15 (1961) 300.
13. H Ashassi, T.A Aliyev, S Nasiri, R Zareipoor, *Electrochimica Acta*, 52 (2007) 5238.
14. H. Vedage, T.A. Ramanarayanan, J.D. Mumford, S.N. Smith, *Corrosion* 49 (1993) 114.
15. V. A. Alves, A. M. C. Paquim, A. Cavaleiro, C. M. A. Brett, *Corrosion Sci.*, 47 (2005) 2871.
16. Lj. Vracar, D. M. Drazic, *J. Electroanal. Chem.*, 339 (1992) 269.

17. D. M. Drazic, *Modern Aspects of Electrochemistry*, Plenum Press, New York. (1990).
18. N. A. Darwish, F. Hilbert, W. J. Lorentz, H. Rosswag, *Electrochim. Acta*, 18 (1973) 421.
19. B. Y. Fang, R. L. Eadie, W. X. Chen and M. Elboujdaini, *Corr. Eng. Sc. and Tech*, 45 (2010) 302.
20. E. McCafferty, N. Hackerman, *J. Electrochem. Soc.*, 119 (1972) 999.
21. J.L. Crolet, N. Thevenot, S. Nestic, *Corrosion*, 54 (1998) 194.
22. A. Bonnel, F. Dabosi, C. Deslouis, M. Duprat, M. Kedam, B.Tribollet. *J. Electrochem. Soc.*, 130 (1983) 753.
23. A.M. Allam, B.G. Ateya, H.W. Pickering, *Corrosion*, 53 (1997) 284.